Quench front progression in a superheated porous medium: experimental analysis and model development

Andrea Bachrata, Florian Fichot, Georges Repetto, Michel Quintard, Joëlle Fleurot

The 14th International Topical Meeting on Nuclear Reactor Thermal Hydraulics (NURETH-14) Log Number: 128
Hilton Toronto Hotel, Toronto, Ontario, Canada, September 25-29, 2011.

QUENCH FRONT PROGRESSION IN A SUPERHEATED POROUS MEDIUM: EXPERIMENTAL ANALYSIS AND MODEL DEVELOPMENT

A. Bachrata[1], F. Fichot[1], G. Repetto[1], M.Quintard[2,3], and J. Fleurot[1]
[1] Institut de Radioprotection et de Sûreté Nucléaire, Cadarache, France
[2] Université de Toulouse ; INPT, UPS ; IMFT (Institut de Mécanique des Fluides de Toulouse) ; Allée Camille Soula, F-31400 Toulouse, France
[3]CNRS ; IMFT ; F-31400 Toulouse, France
andrea.bachrata@irsn.fr, florian.fichot@irsn.fr, georges.repetto@irsn.fr, michel.quintard@imft.fr

Abstract

In case of severe accident in a nuclear reactor, the fuel rods may be highly damaged and oxidized and finally collapse to form a debris bed. Removal of decay heat from a debris bed is a challenging issue because of the difficulty for water to flow inside. Currently, IRSN has started experimental program PEARL with two experimental facilities PRELUDE and PEARL, to investigate the reflood process at high temperature, for various particle sizes. On the basis of PRELUDE experimental results, the thermal hydraulic features of the quench front have been analysed and the intensity of heat transfers was estimated. From a selection of experimental results, a reflooding model was improved and validated. The model is implemented in the code ICARE-CATHARE developed by IRSN which is used for severe accident reactor analysis.

1. Introduction

In case of severe accident in a nuclear reactor, water sources are not available for a long period of time and the reactor core heats up due to the residual power. This leads to cladding oxidation and, possibly, to the collapse of fuel rods and melting of reactor core materials that can result in the formation of a “debris bed”. In a debris bed, the particles size would be a few millimeters (characteristic length-scale: 1 to 5 mm). If the core cannot be cooled down, core melting and melt relocation to the lower plenum occurs. If the lower plenum is dry, the hot materials in contact with the vessel might endanger the integrity of the reactor pressure vessel wall. The aim of the severe accident management is to prevent the development of the above-mentioned scenario to more serious conditions. From a safety point of view, it is important to evaluate chances of coolability of the reactor core during a severe accident. This is in line with the safety philosophy of defence in depth which requires to foresee and to analyse all options to stop an accident at any stage.

Reflooding (injection of water) is possible if one or several water sources become available during the accident. An efficient use of those water sources may significantly contribute to the extension of safety margin of pressurized water reactors. If water source is available during the late phase of accident, water will enter a configuration of the reactor core that is largely modified and will resemble to the debris bed observed in TMI-2. The higher temperatures and smaller hydraulic diameters in a debris bed make the coolability more difficult than for intact fuel rods under LOCA conditions. However, the successful reflood of such a severely damaged reactor core already happened during the TMI-2 accident [1]. On the other hand, it must also be recognized that at elevated core temperatures, the rate of oxidation of metals may be very high if steam is available.

Therefore, reflood is likely to lead to an enhanced hydrogen formation and the risk of containment damage. The prediction of the core evolution in case of reflood requires an accurate modelling of both the heat transfer and the oxidation of metal (possibly molten). Thus, the reflood scenario of a severely damaged reactor core represents actually one of the major objectives of severe accident research. The present paper will only deal with the heat transfer issue.

2. Experimental data

The available knowledge about debris bed reflooding comes from a few experimental programs that were performed in the past 30 years. Among them, the experiments of Tutu et al. [3] and Tung and Dhir [7] have helped understanding the progression of the quench front and the production of steam during quenching. Currently, the French Institut de Radioprotection et de Sûreté Nucléaire (IRSN) sets up two experimental facilities, PRELUDE and PEARL (in 2012) to enhance the database of tests results. The main objectives are to extend the range of thermal-hydraulic conditions to higher temperatures and higher pressures than in previous tests [2], [3]. The objective is also to study 2D/3D effects during quenching. The PRELUDE experiment [4] is a preliminary test section, with smaller dimensions and running only at atmospheric pressure. That facility is used to optimize the induction heating and the measurement devices that should be used in PEARL facility. The PRELUDE geometry (Figure 1) consists of a cylinder with an internal diameter of 174 mm filled with spherical steel particles of 4, 2 or 1 mm. The height of the debris bed is fixed to 200 mm and the porosity is 0.4. The debris bed is brought to its initial temperature by inductive heating that is maintained during reflood. The initial temperature is 400°C or 700°C or 1000°C. The outlet pressure is 1 bar. Liquid water is injected at 20°C at the bottom of the debris bed. Four inlet superficial velocities were used, namely 0.555, 1.38, 2.77 and 5.55 mm/s.

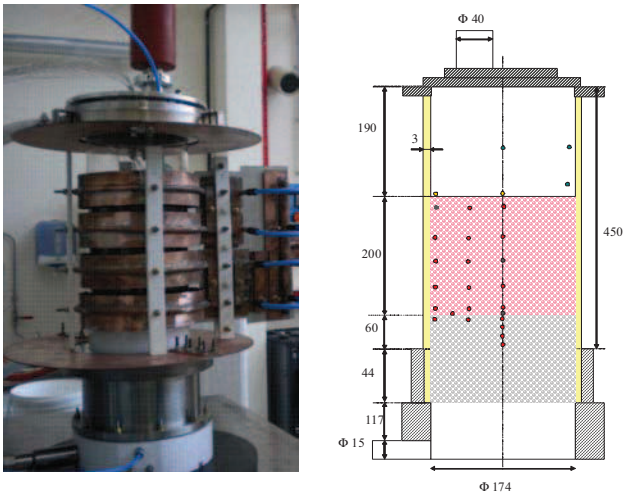

Figure 1 PRELUDE experimental facility (dimensions in mm)

The particle and fluid temperatures are measured at different positions. The steam flow is measured at the inlet and the outlet of the section and the difference of pressure across the particle bed is also measured. Reproducibility tests have been performed and have shown that outstanding disturbances observed in some measurements are not produced randomly but are reproduced for every test. Therefore, those disturbances result only from local non-homogeneities of the debris

bed. The analysis presented in this paper concerns the PRELUDE tests with initial temperature 400°C. We assume that the largest steam production occurs in the areas where the temperature is well below 400°C, so a particular attention to modelling of heat transfer in that zone was done.

2.1 Analysis of experimental results

The velocity of the quench front is one of the key parameters to be validated in reflood analysis. First, the conditions of existence of a steady-state progression have to be analysed. It is interesting to study if a steady-state progression occurs because this will significantly help in future analysis of large scale and simplification of model. Moreover, when the steady-state progression exists, its velocity may be used to correlate some relevant parameters characterizing the particle bed or the water injection. The basic phenomenology that is summarized in this section comes from the interpretation of PRELUDE bottom-reflood experimental results. First, water enters the porous media that is initially at high temperature (e.g. 300-600°C above the quenching temperature). The initial heat transfer and evaporation rate are low because the heat transfer coefficient is low due to film boiling. As water continues to progress the first quenching of particles occurs at the bottom and thus, high evaporation rate occurs. From there, the quenching front starts to progress, initially with a velocity that is close to water injection velocity and, later, at a lower constant velocity (for most of the tests). The analysis of experimental data never showed a quench front velocity that was larger than the water injection velocity. The peak of steam production if it occurs (Figure 2), will results from that maximum initial quench front velocity and from the accumulation of water in the porous column. The similar behavior in a steam flow production was already observed in previous studies [3] but the measurements were not so accurate. When the progression becomes stable, the position of the quench front corresponds roughly to a balance between the cumulated evaporation rate downstream of the quench front position and the local water flow rate.

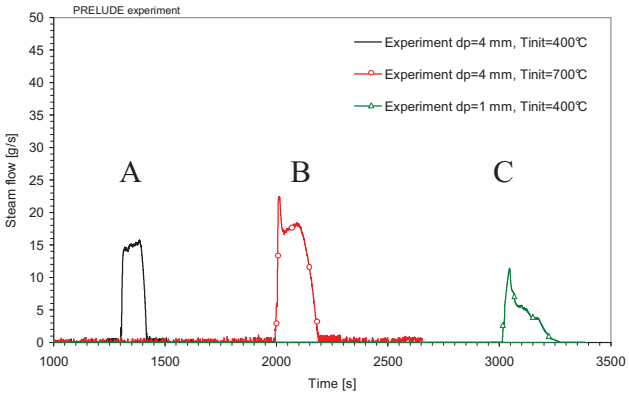

Figure 2 Examples of steam flow production during reflood at different PRELUDE tests

2.1.1 Steady state progression of quench front

The quench front velocity is identified from the determination of the elevation where temperature is below the saturation temperature. It may be evaluated within the column for three different radii and five different elevations (see Figure 1). It should be noted that the accuracy on the instant of quenching depends on the reference temperature that is taken for comparison. On Figure 3 (left)

we can see that the saturation temperature is not a good reference because it is measured with some error (few degrees) and is not always stable. In order to be more accurate, it is better to take T_{sat}+5 or T_{sat}-5 as a reference temperature but the optimal value is not decided.

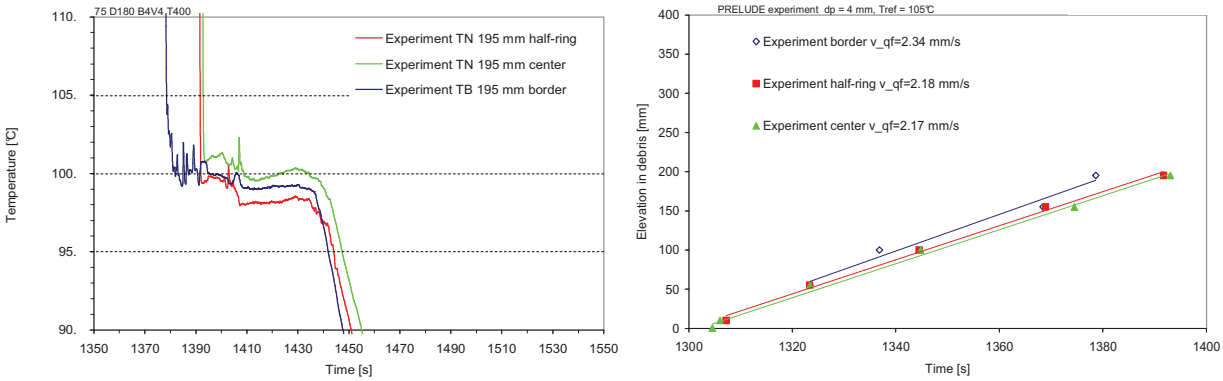

Figure 3 Identification of quench front velocity

Analyzing the PRELUDE experimental results we can conclude that there exists a steady state propagation of the quench front for all the cases considered here (see Section 4.1). It indicates that the dynamic processes occurring in the bed are "fast" with respect to the injection velocity (no significant delay of quenching) but "stable" (no acceleration or dramatic increase of steam production). The quench front velocity is the same for the central and mid-radius positions. It is faster near the wall, probably because the initial temperature is lower and the porosity slightly higher. In the next section we will see that the steady state propagation of the quench front allows a simpler analysis of model and experimental measurements.

2.1.2 Conversion factor between produced steam and injected water

If there is a steady state propagation of the quench front, some balance equations may be simplified and some variables can be expressed as a function of the propagation velocity. The conversion factor between the produced steam flow and the injection liquid flow (Q_g/Ql) is of particular interest. Adapting the formulations of Tutu et al. [3] and Tung and Dhir [7], the energy balance is written as:

$$\frac{Q_g}{Q_l} = \frac{v_{QF}(1-\varepsilon)\rho_s Cp_s(T_s - T_{sat}) + v_l(1-\varepsilon)\rho_s Cp_s(T_{sat} - T_l) - v_l\rho_l\varepsilon Cp_l(T_{sat} - T_l)}{\left[\Delta h^{vap} + Cp_g(T_s - T_{sat})\right]v_l\rho_l\varepsilon} \quad (1)$$

where v_{QF} is the velocity of progression of quench front and T_s is the initial temperature of solid. From Eq. (1) we can see that there exists a simple relation between the quench front velocity and the conversion factor. On Figure 4 (right) it is clear that the measured quench front velocity is always lower than the liquid injection velocity. On Figure 4 (left) we compare the experimental and calculated (Eq. (1)) conversion factors. The experimental conversion factors are presented only for test cases where a steady-state steam production was identified e.g. cases A and B in Figure 2. We can see that the experimental conversion factors are higher than calculated. This may be due to the fact that, the quench front velocity identified in the centre was taken to calculation but for most of the cases the quench front velocity at border was higher so the conversion factor is expected to be higher.

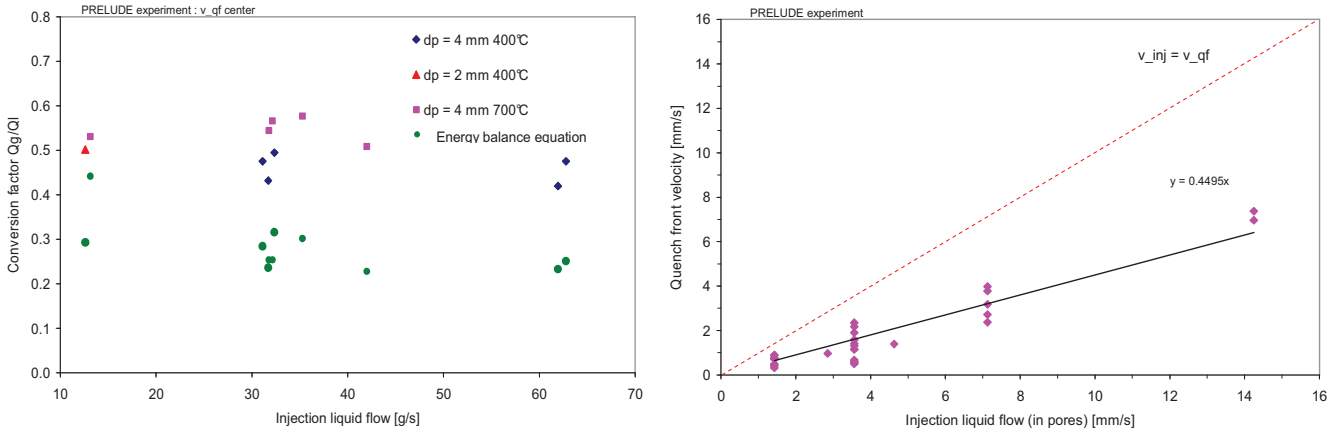

Figure 4 Conversion factor (left) and quench front velocities for different tests (right)

In PRELUDE experiments, the difference of pressure over the height of porous medium was recorded. Following the division of the porous medium into three zones (see Figure 5) we can identify three different contributions:

- Quenched zone: is the zone from z_0 to z_1. Its contribution to the pressure difference follows Darcy's law for the single phase liquid flow. As the liquid velocities are small (few mm/s), the largest contribution to the pressure difference in that zone is the hydrostatic pressure.
- Two-phase flow zone: is the zone from z_1 to z_2, where both liquid and steam are present. In this zone, the pressure difference follows the generalized Darcy's laws for two-phase flows through porous media (see Eqs. (3) and (4) below).
- Gas single phase zone: is the zone from z_2 to H, where only steam is present. However, the liquid could be present as droplets if sufficient entrainment occurs. In some tests, the presence of liquid at the top of porous medium was observed/calculated before the porous medium was completely quenched. In case of gas single-phase flow, the pressure difference follows the Darcy/Ergun law (because of higher Reynolds numbers than for the liquid flow). The gas flow velocity can be directly calculated from the steam flow measured at the top of the experimental facility.

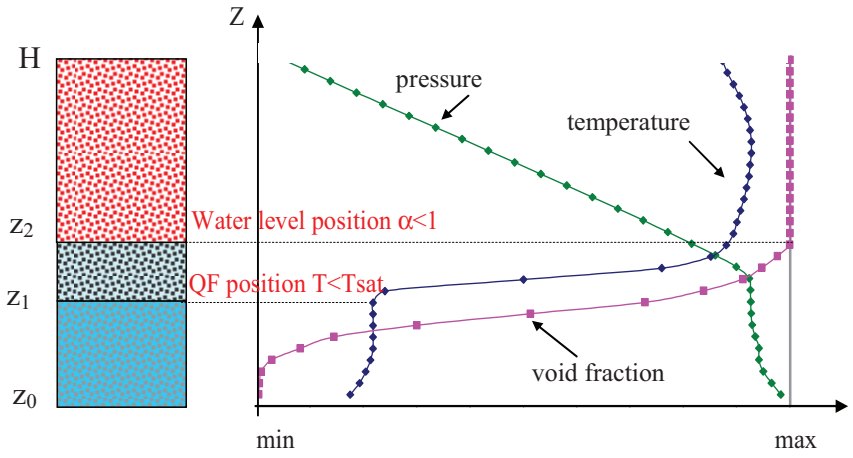

Figure 5 Different zones during reflood

In PRELUDE experiments, pressure difference between z_0 and H is recorded. Assuming that the liquid progresses with the quench front velocity (identified from temperature measurements), we can eliminate the contribution of hydrostatic pressure. From that simple analysis, we observe that the pressure may be fitted by a linear function (see Figure 6 left), thus we can write:

$$\frac{dP}{dt} = v_{QF}\frac{dP}{dz} = a \tag{2}$$

where v_{QF} is the quench front velocity, P is the pressure and a is a fit from linear regression of pressure curve. We can conclude that the pressure drop is proportional to the height of the still unquenched bed and thus, the pressure difference decreases with time, as the quench front progresses. Applying Eq.(2), we can find directly the dependence of the pressure difference on the quench front velocity. We can identify the pressure difference for each test and to show its dependence e.g. on the gas flow velocity (Figure 6 right). Further analysis of pressure losses are a matter of current investigation. In order to identify pressure losses coefficients, more temperature measurements and local pressure measurements are needed.

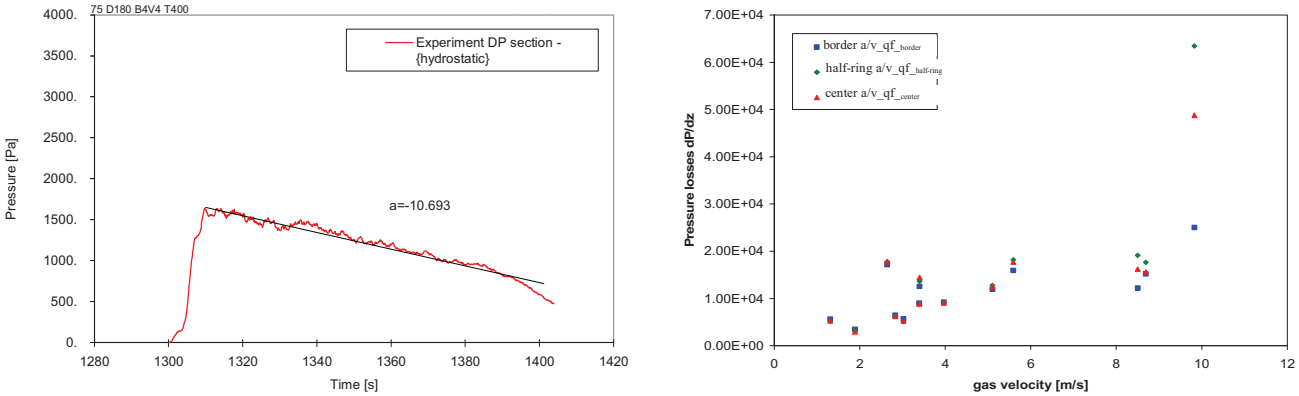

Figure 6 No-hydrostatic contribution to pressure difference for different tests with dp = 4 mm

3. Modelling of the reflood process

In this section, experimental results are used to validate a reflood model. Such a model for the three-dimensional two-phase flow in a heat-generating porous medium was earlier developed and assessed [6], [8], [9]. This model is recalled here, with some improvements.

3.1 Momentum balance equations

The friction forces between the solid matrix and the fluid phases are taken into account by using the classical extension of Darcy's law to two-phase flows. This means that viscous and inertial drag forces are calculated with relative permeabilities and passabilities coefficients, depending mainly on the void fraction using standard Brooks and Corey relation [20]. There is no explicit interfacial drag force between the liquid and gas phases. This may be missing in the model, as it was suggested by [10], but there does not appear to be a satisfactory correlation available in the literature. Therefore, the momentum balance equations have a rather classical form, as follows:

$$\alpha\langle\rho_g\rangle^g\left(\frac{\partial\langle v_g\rangle^g}{\partial t}+\langle v_g\rangle^g.\nabla\langle v_g\rangle^g\right)=-\alpha\nabla\langle p_g\rangle^g+\alpha\langle\rho_g\rangle^g g-\varepsilon\alpha^2\left(\frac{\mu_g}{Kk_{rg}}\langle v_g\rangle^g+\varepsilon\alpha\frac{\langle\rho_g\rangle^g}{\eta\eta_{rg}}\langle v_g\rangle^g\left|\langle v_g\rangle^g\right|\right) \quad (3)$$

$$(1-\alpha)\langle\rho_l\rangle^l\left(\frac{\partial\langle v_l\rangle^l}{\partial t}+\langle v_l\rangle^l.\nabla\langle v_l\rangle^l\right)=-(1-\alpha)\nabla\langle p_l\rangle^l+(1-\alpha)\langle\rho_l\rangle^l g-\varepsilon(1-\alpha)^2\left(\frac{\mu_l}{Kk_{rl}}\langle v_l\rangle^l+\varepsilon(1-\alpha)\frac{\langle\rho_l\rangle^l}{\eta\eta_{rl}}\langle v_l\rangle^l\left|\langle v_l\rangle^l\right|\right) \quad (4)$$

In these equations, $\langle p_\beta\rangle^\beta, \langle\rho_\beta\rangle^\beta, \mu_\beta$ and $\langle v_\beta\rangle^\beta$ are respectively the intrinsic average pressure, density, dynamic viscosity and velocity of the β-phase ($\beta = g, l$). For uniform spherical particles, the intrinsic permeability and passability are correlated with the particle diameter d_p and the porosity ε by the Carman-Kozeny relation [11] and Ergun law [12]. The capillary pressure is introduced in the equations to represent macroscopically the effect of the pressure jump across the non-wetting/wetting phase interface.

3.2 Energy balance equations

Macroscopic energy conservation equations for the three phases are obtained by averaging the local energy conservation equations [13], [14]. The complete set of closure problems is presented in [13]. The averaged equations are simplified following [15] and the resulting macroscopic energy conservation equations are expressed as follows:

- gas phase $$\frac{\partial\left(\alpha\varepsilon\langle\rho_g\rangle^g\langle h_g\rangle^g\right)}{\partial t}+\nabla.\left(\alpha\varepsilon\langle\rho_g\rangle^g\langle v_g\rangle^g\langle h_g\rangle^g\right)=\nabla.\left(K_g^*\nabla.\langle T_g\rangle^g\right)+\dot{m}_g h_g^{sat}+Q_{pg}+Q_{gi} \quad (5)$$

- liquid phase $$\frac{\partial\left((1-\alpha)\varepsilon\langle\rho_l\rangle^l\langle h_l\rangle^l\right)}{\partial t}+\nabla.\left((1-\alpha)\varepsilon\langle\rho_l\rangle^l\langle v_l\rangle^l\langle h_l\rangle^l\right)=\nabla.\left(K_l^*\nabla.\langle T_l\rangle^l\right)+\dot{m}_l h_l^{sat}+Q_{pl}+Q_{li} \quad (6)$$

- solid phase $$\frac{\partial\left((1-\varepsilon)\langle\rho_s\rangle^s\langle h_s\rangle^s\right)}{\partial t}=\nabla.\left(K_s^*\nabla.\langle T_s\rangle^s\right)-Q_{pl}-Q_{pg}-Q_{pi}+\omega_s \quad (7)$$

In these equations, $\langle h_\beta\rangle^\beta$ and $\langle T_\beta\rangle^\beta$, are the macroscopic enthalpy and the temperature of the β-phase respectively ($\beta = g, l, s$ for the gas, liquid and the solid phases). K_β^* is the effective thermal diffusion tensor including dispersion. The thermal exchanges between fluid phase and solid phase ($Q_{p\beta}$), fluid phase and interface ($Q_{\beta i}$) and solid phase and interface (Q_{pi}) are expressed as a heat transfer coefficient multiplied by the temperature difference. The phase change rate is given by the relation:

$$\dot{m}_g=\frac{Q_{pi}-Q_{gi}-Q_{li}}{h_g^{sat}-h_l^{sat}} \quad (8)$$

3.3 Improvement of the heat transfer model

The porous medium temperature at the time of water injection may be significantly higher than the rewetting temperature and complicated flow and heat transfer patterns are generated. At high surface temperatures corresponding to film boiling (Figure 7), the cooling rate is rather low as the liquid is separated from the surface by a continuous vapor film. As temperature decreases below

the minimum heat flux temperature (usually called Leidenfrost), a transition boiling regime is encountered, where an intermittent wetting of the surface occurs and the heat transfer rate increases with decreasing surface temperature. At a surface temperature corresponding to critical heat flux, the entire surface becomes available for wetting and intense nucleate boiling ensues, causing the surface to cool rapidly until the saturation temperature is reached, below which the surface is cooled by single-phase liquid convection. In our model, specific heat transfer coefficients were obtained analytically in simplified geometrical configurations as the stratified cell and Chang's cell [13]. For a stratified unit cell, two typical phase repartitions were considered, namely the *solid-liquid-gas* and the *solid-gas-liquid* repartition. The first refers to liquid being the wetting phase, the second refers to vapor being the "wetting" phase. As for the flow through the porous medium, we assume that the flow structure can correspond to a distribution in channels [16]. We assume that, for an oriented liquid flow in porous media, we can expect a phase repartition where one phase will be "wetting" and the second phase will eventually flow in the remaining pores under the form of bubbles or slugs. Because of this assumption, the effective properties obtained for a stratified unit cell are combined in our model. However, the stratified flow assumed in our model is applicable mostly in the case of film condensation (below saturation temperature) or film boiling (above Leidenfrost temperature) only. Consequently, an improvement of the model is proposed for the nucleate boiling and transition boiling regimes (Figure 7 left), where the heat flux depends on bubble nucleation, which is not taken into account in the existing model. The extension of the model which is proposed comes from the theory of flow boiling in small hydraulic diameter channels. Recent studies [17] concluded that neither the nucleate boiling nor turbulent convection are the controlling mechanisms in minichannels. The important process seems to be a transient thin film evaporation where the minichannel flows are typically laminar [18]. Under such conditions, our model describes this thin film evaporation but it is proposed to enhance it by introducing a term of nucleate boiling as follows:

$$h = (1-\alpha^n)h_{nb} + \left((1-\alpha)h_{cv,l} + \alpha h_{cv,g}\right) \tag{9}$$

where h is the heat transfer coefficient applied in expression for a specific thermal exchange (equations (5)-(7)) and exponent n was a matter of investigation in a range (1 to 5). Using the above mentioned equation, the nucleate boiling will be strongly reduced with an increase of vapor quality, which inhibits bubble growth and leads to dry-out at high vapor qualities.

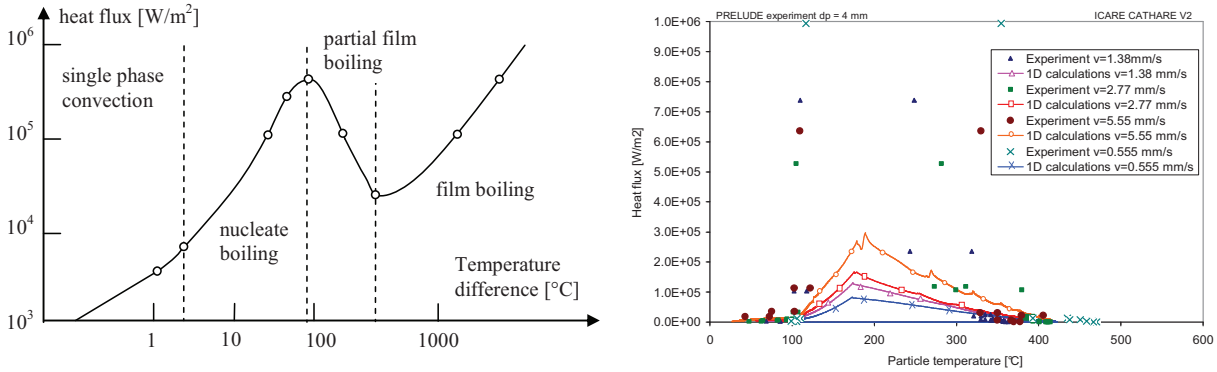

Figure 7 Nukiyama flow boiling curve (left), experimental/calculated results (right)

Secondly, heat transfers in the transition zone were also modified. From the PRELUDE measurements of particle temperature, the transition boiling heat fluxes may be estimated as a function of particle temperature. We can obtain the heat flux using the formula:

$$Q = \frac{mC_p}{S}\frac{dT}{dt} - \frac{Q_s}{S} \tag{10}$$

where m is the weight of the particle where the thermocouple is located, S is its surface, and Q_s is the maintained volumetric power during reflood. Therefore the profile and intensity of heat transfer may be reconstructed along the transition boiling range (Figure 7 right). From the experimental results, it is observed that the maximum heat flux reached values in the range of 500-1000 kW/m^2. Compared to experimental results, the calculated heat flux reached lower values. On the other hand, the calculated heat flux reaches yet important values (>10^5 W/m^2). It is important to note that the experimental heat fluxes presented in Figure 7 (right) are measured locally where the calculated heat fluxes are averaged for whole mesh volume and as expected, reach lower values. Secondly, from the experimental results, it is not possible to determine the temperature where the maximum heat flux (CHF) is achieved because it occurs over a very narrow temperature range (about 10K). Currently, there is still a lack of information about the critical heat flux in porous media during reflood. Our model, in the absence of specific determination for porous media, uses the Groenveld critical heat flux correlation [19] including its dependence on the hydraulic diameter. In order to describe the increasing heat transfer with decreasing surface temperature, a simple cubic dependence on surface temperature was prescribed. The form of the dependence on the surface temperature (parameter ξ) and void fraction (parameter n) was the matter of a sensitivity study. Currently, the heat flux dependence on void fraction is expressed as:

$$Q = (1-\alpha^n)(1-\xi)Q_{CHF} + \xi(1-\alpha)Q_{cv,g} \tag{11}$$

If the solid temperature reaches the critical heat flux temperature, the heat exchange in Eq. (11) is reduced to that is expressed in Eq. (9), thus the nucleate boiling regime follows. The calculations presented in this paper uses the exponent $n=2$.

4. Implementation in the ICARE-CATHARE reflood model

ICARE-CATHARE [5] is a computer code developed by IRSN, designed to describe accurately light water reactor accidental sequences up to a possible vessel failure. It involves advanced models (two-phase multi-dimensional thermal-hydraulics and degradation models) and is built from the coupling of the thermal-hydraulics code CATHARE to the severe accident code ICARE. The above-presented two-phase flow model is implemented in this code. The constitutive heat transfer relations are described in terms of a unique boiling curve (Figure 7) from which the code selects the appropriate heat transfer coefficients for both phases (vapor/liquid). For instance, the minimum film stable temperature was set to 400°C and, mostly, the transition zone and nucleate boiling regime were validated with experimental results.

4.1 Validation of model with PRELUDE data

The ICARE-CATHARE 1D reflood calculations were performed for PRELUDE tests with initial debris bed temperature at 400°C. The steel particles are placed above a bed of quartz particles, installed in the PRELUDE facility in order to avoid placing a metallic grid which would heat-up

because of induction. The homogeneously distributed mass power was set to 210, 170 or 70 W/kg depending on particle diameter. The calculations were performed at atmospheric pressure and for different bottom liquid flow injections (0.555, 1.38, 2.77 and 5.55 mm/s). The temperature of injected water was 20°C. The objective of the calculations was to validate the model in the prediction of heat fluxes, progression of quench front and steam formation, but also to determine the extent and structure of the two-phase region, for which no information can be deduced from the measurements. In Figure 7 (right), it is observed that, from the experimental results, the maximum heat flux reached values in the range of 500-1000 kW/m^2. Compared to experimental results, the calculated heat flux reached lower values. However, the calculated heat flux is sufficiently high (>10^5 W/m^2) to allow rapid quenching thus the quench front velocity and steam production are well predicted.

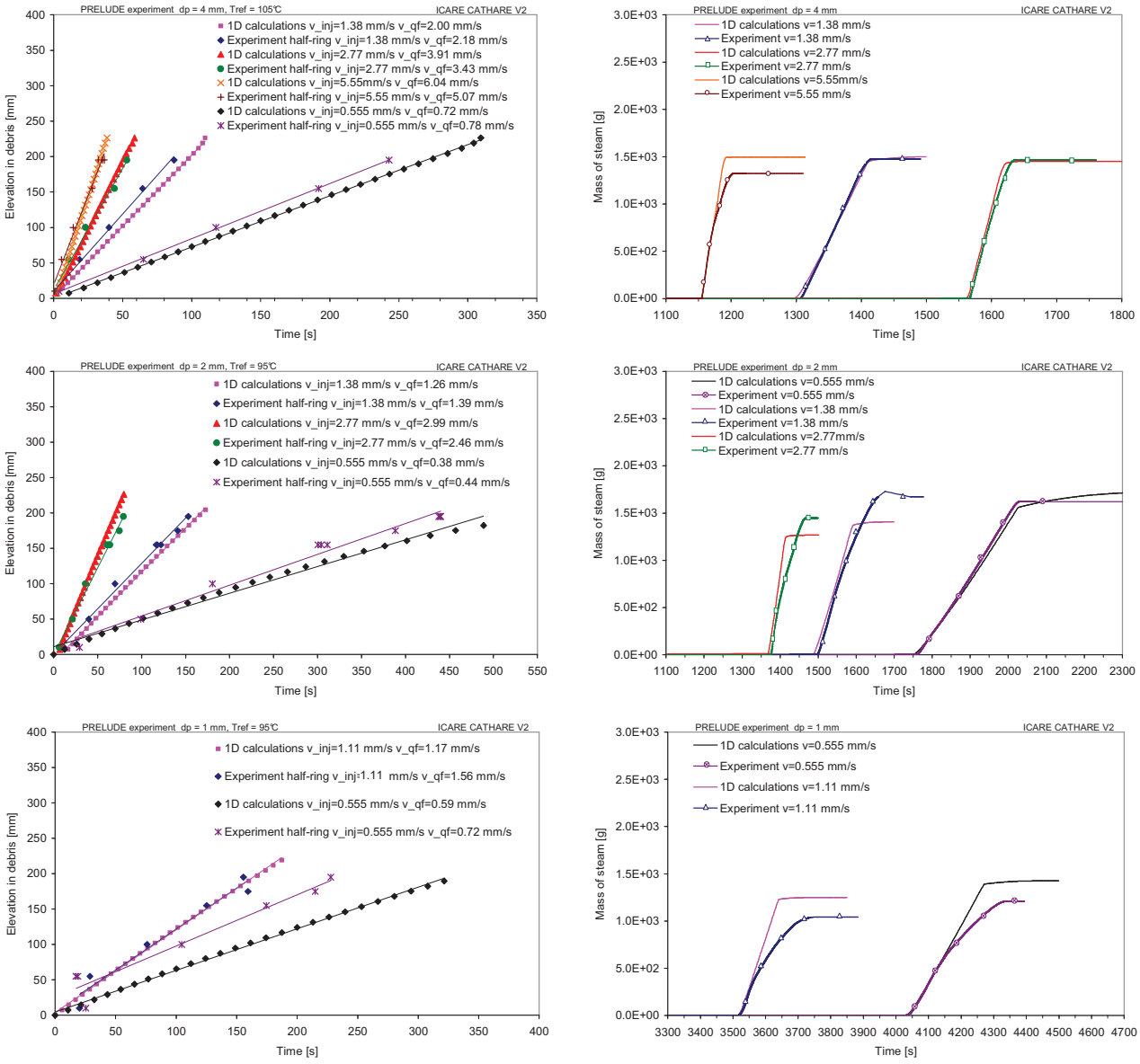

Figure 8 Quench front velocity (left) and cumulated mass of steam (right)

On Figure 8 (left), we can see that the calculated quench front progression is in good agreement with experimental results for the whole range of liquid injection velocities and particle diameters. Limited discrepancies are observed for the lowest velocity (0.555 mm/s) and 1 mm particles. However, in this test the quench front velocity at border was higher compared to other rings so the 2D calculations of this test are ongoing. On Figure 8 (right) the cumulated mass of steam for different tests is plotted as a function of time. From the curve slopes, we can see that the time interval in which steam is produced decreases when the injection velocity of liquid increases. This affects the pressure peak which reaches higher values for higher liquid flows (not shown here). On the other hand, the total amount of produced steam is lower. However, at higher injection velocities water bypassed through the lateral region. When it reached the top of the bed, the steam was partly condensed and the measurements could be influenced. From the calculation results we can see that the slope of the curve for each test corresponds well to experimental results. The differences in the final steam production is attributed to different initial conditions (temperature is not perfectly uniform in the experiment).

5. Conclusions

The first series of PRELUDE tests has confirmed some of the previous experimental results. Moreover, the results brought new data that contribute to understanding of quenching of a particle bed with bottom cooling injection. The presented analysis concern the experiments with the debris bed formed with 4, 2 or 1 mm particles. The initial temperature was 400°C. The liquid flow injection at the bottom of test section was 0.555, 1.38, 2.77 or 5.55 mm/s. First, the existence of a quasi steady propagation of the quench front is verified for all tests. The quench front velocity depends mainly on the injection velocity and is almost independent of the particle diameter. It is confirmed by both the temperature and pressure measurements. The intensity of heat fluxes was estimated from measurements. This helped to improve the modelling of heat transfers in the transition boiling regime. Comparisons of temperature evolutions at different elevations show that the model is able to predict quenching velocity for different inlet flow rates and different particle diameters, in the whole range covered by PRELUDE experiments. The steam production is also in agreement with experimental results. Calculations clearly show the propagation of a two-phase quench front separating the superheated steam region and the subcooled water region. After a transient evolution resulting in a peak of the quench front velocity, the evolution is steady.

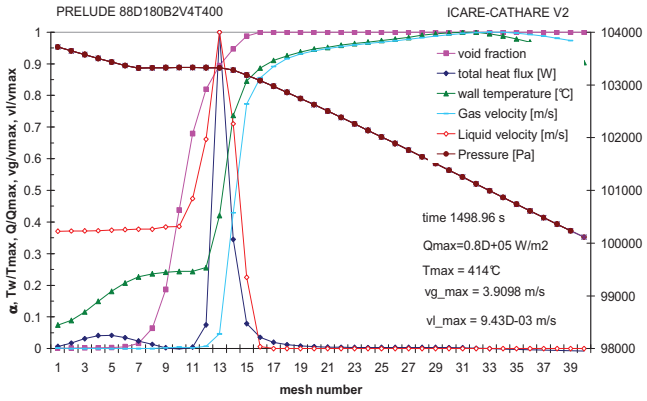

Figure 9 Additional calculations for local parameters that were not measured

Moreover, the analysis of calculations for different parameters that cannot be measured allow to draw supplementary conclusions (Figure 9). The thickness of the two-phase region was observed to be few centimetres and appeared to be almost constant during the propagation. The void fraction at the maximum heat flux was observed to reach high values (0.7-0.9). The liquid flow velocity increased before quenching, however the maximum values were small (below 1 cm/s). The calculations of local pressure identified a changing of slope at the quenching position. If this result is confirmed by the future tests with local pressure measurements, the additional information at quenching can be revealed.

Acknowledgment

The SARNET 2 project of the 7th European framework program is gratefully acknowledged for the transfer knowledge assessment and financial support of debris bed reflooding studies.

6. References

[1] C. Müller, "Review of debris bed cooling in the TMI-2 accident", Nuclear Engineering and Design, Vol. 236, 2006, pp. 1965-1975.
[2] T. Ginsberg, et al, "An experimental and analytical investigation of quenching of superheated debris beds under top reflood conditions", Report NUREG/CR-4493, 1986.
[3] Tutu, et al., "Debris bed quenching under bottom flood conditions", Report NUREG/CR-3850, Sandia National Labs, 1984.
[4] G. Repetto, et al., "Experimental program on debris reflooding (PEARL) - Results on PRELUDE facility", (NURETH14), Toronto, Canada, 2011 September 25-29.
[5] V. Guillard, el al., "ICARE-CATHARE coupling: three dimensional thermal-hydraulics of severe LWR accidents", Proceeding of ICONE-9, Nice, France, 2001.
[6] F. Duval, F. Fichot and M. Quintard, "A local thermal non-equilibrium model for two-phase flows with phase change in porous media", International Journal of Heat and Mass Transfer, Vol. 47(3), 2004, pp. 613-639.
[7] V.X. Tung and V.K Dhir, "Quenching of a hot particulate bed by bottom quenching", Proc. of ASME-JSME Thermal Engineering Joint Conference, Honolulu, Hawaï, 1983.
[8] N. Trégourès, F. Fichot, F. Duval, M. Quintard, "Multi-dimensional numerical study of core debris bed reflooding under severe accident conditions", Proceeding of 10th International Topical Meeting on Nuclear Reactor Thermal Hydraulics, Seoul, Korea, 2003.
[9] F. Fichot, et al., "Multi-dimensional approaches in severe accident modelling and analyses", Nuclear Engineering and Design, Vol. 38(8), 2006, pp. 733-752.
[10] T. Schulenberg and U. Müller, "An improved model for two-phase flow through beds of coarse particles", Int. J. Multiphase Flow, Vol. 13(1), 1987, pp. 87-97.
[11] P. C. Carman, "The determination of the specific surface area of powder", I. J. Soc. Chem. Ind, Vol. 57, 1937, pp. 225-234.
[12] S. Ergun, "Fluid flow through packed columns", Chem. Eng. Prog., Vol. 48, 1952, pp. 89-97.
[13] F. Duval, "Modélisation du renoyage d'un lit de particules: contribution à l'estimation des propriétés de transport macroscopiques", PhD thesis, INPT, Toulouse, France, 2002.

[14] M. Quintard, M. Kaviany and S. Whitaker, "Two-medium treatment of heat transfer in porous media: Numerical results for effective properties", Advances in Water Resources, Vol. 20(2-3), 1997, pp. 77-97.
[15] F. Petit, et al., "Ecoulement diphasique en milieu poreux: Modèle à non-equilibre local", Int. J. Therm. Sci, Vol 38, 1999, pp. 239-249.
[16] V. X. Tung and V. K. Dhir, "A hydrodynamic model for two-phase flow through porous media", Int. J. Multiphase Flow, Vol. 14, 1988, pp. 47-65.
[17] J. R. Thome, "Boiling in microchannels: a review of experiment and theory", Int. J. of Heat and Fluid Flow, Vol. 25, 2004, pp. 128-139.
[18] A. Mukherjee, "Contribution of thin-film evaporation during flow boiling inside microchannels", Int. J. of Thermal Sciences, Vol. 48, 2009, pp. 2025-2035.
[19] M. Bazin and M. Pellissier, "Description of the base revision 6.1 physical laws used in the 1D, 0D and 3D modules", Technical report SSTH/LDAS/EM/2005-038, 2006.
[20] R. H. Brooks and A. T. Corey, "Properties of porous media affecting fluid flow", J. Irrig. Drain. Div. Am. Soc. Civ. Engrs IR2, Vol. 92, 1996, pp. 61-89